

# Host-Guest Systems on the Surface of Functionalized Superparamagnetic Iron Oxide Nanoparticles (SPIONs) Utilizing Hamilton Receptors and Cyanurate Derivative Molecules

Muhammad Ali,<sup>[a]</sup> Evgeny Kataev,<sup>[a]</sup> Johannes Müller,<sup>[a]</sup> Hyoungwon Park,<sup>[b]</sup> Marcus Halik,<sup>[b]</sup> and Andreas Hirsch<sup>\*[a]</sup>

*In memoriam to Prof. Klaus Hafner.*

**Abstract:** The study of hydrogen bonding interactions at the level of functionalized nanoparticles remains highly challenging and poorly explored area. In this work, superparamagnetic iron oxide nanoparticles (SPIONs) were orthogonally functionalized using receptors bearing multiple hydrogen bonding motifs. Pristine SPIONs were modified by wet chemical processes with Hamilton receptors (hosts), or cyanurate-guest molecules linked to phosphonic acid moieties for monolayer functionalization. The modified surfaces were fully characterized and the number of attached ligands on the surface were determined. The host-guest interactions on the interface of

modified SPIONs were investigated by using UV-Vis spectroscopic titrations. Functionalized SPIONs demonstrated two to three magnitudes stronger binding affinities as compared to the related molecular interactions in solution due to synergistic effects on complex surface environment. Higher supramolecular binding ratios of host-guest interactions on the modified surface were emerged. These studies provide fundamental insights into supramolecular complexations on the surface at solid-liquid interface systems with applications in engineered nanomaterials, nano-sensing devices, and drug delivery systems.

## Introduction

In recent years, superparamagnetic iron oxide nanoparticles (SPIONs) have been extensively explored in various applications.<sup>[1]</sup> Large specific surface area combined with magnetic response properties offer versatile approaches to engineer, exploit and utilize the SPIONs in many fields such as nano-catalysts,<sup>[2]</sup> smart materials for remediation,<sup>[3]</sup> and medical nano-engineering.<sup>[4]</sup> The superparamagnetic nanoparticles were often used as solid core materials, where functional organic

materials, anchored on the surface, rendering the surface properties. In addition, the superparamagnetic properties give an easy access to collect the nanoparticles out from the working systems by simply applying an external magnetic field. The surface modification of nanoparticles can improve the reactivity,<sup>[5]</sup> dispersability,<sup>[6]</sup> biocompatibility,<sup>[7]</sup> and multifunctionality<sup>[8]</sup> thus, broadening the potential applications. The surface of SPIONs can be potentially functionalized with host or guest molecules in order to study a collective behavior of such functionalized particles towards multiple recognition events of desired molecules or even complementary particles. This host-guest chemistry at the level of nanoparticles remains completely unexplored; however, it opens a great perspective to realize such processes as signal amplification, directed self-assembly of nanoparticles and energy storage.

Hydrogen bonding interactions between Hamilton receptors and cyanurate or barbiturate derivatives are excellent model systems with association constants ( $K_a$ ) ranging from  $10^3$  to  $10^6 \text{ M}^{-1}$ .<sup>[9]</sup> These interactions have been applied to realize charge transfer interactions,<sup>[10]</sup> light-driven rotaxane systems,<sup>[11]</sup> self-assembled architectures,<sup>[12]</sup> and sensory devices.<sup>[13]</sup> Several attempts to attach Hamilton receptor to the surface of nanoparticles have been reported. However, they lack detailed investigations of host-guest interactions on the interface of modified nanoparticles.<sup>[14]</sup> Zeininger et al. used catechol-Hamilton receptor conjugate to modify the surface of ZnO nanorods and studied the sedimentation behavior in chloroform, while Hasenoehrl et al. reported thiol-Hamilton receptor molecules to

[a] M. Ali, Dr. E. Kataev, J. Müller, Prof. Dr. A. Hirsch  
Department of Chemistry & Pharmacy  
Chair of Organic Chemistry II  
Friedrich Alexander University of Erlangen-Nuremberg  
Nikolaus-Fiebiger-Strasse 10, 91058 Erlangen (Germany)  
E-mail: andreas.hirsch@fau.de

[b] H. Park, Prof. M. Halik  
Organic Materials and Devices  
Department of Materials Science  
Interdisciplinary Center for Nanostructured Films (IZNF)  
Friedrich Alexander University of Erlangen-Nuremberg  
Cauerstrasse 3, 91058 Erlangen (Germany)

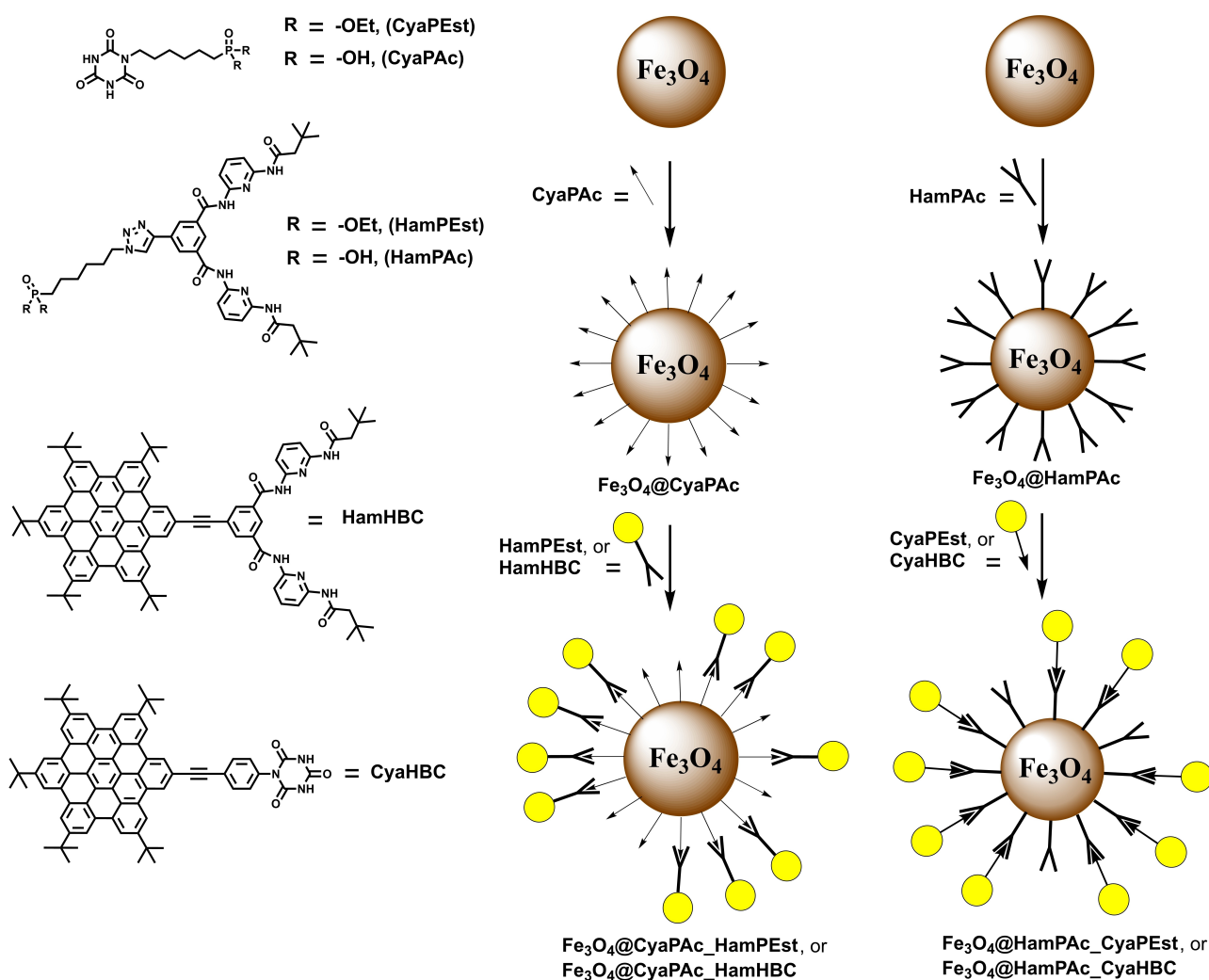
Supporting information for this article is available on the WWW under <https://doi.org/10.1002/chem.202102581>

© 2021 The Authors. Chemistry - A European Journal published by Wiley-VCH GmbH. This is an open access article under the terms of the Creative Commons Attribution Non-Commercial NoDerivs License, which permits use and distribution in any medium, provided the original work is properly cited, the use is non-commercial and no modifications or adaptations are made.

functionalize gold nanoparticle. Binder utilized click-chemistry to attach barbiturates on luminescent CdSe nanoparticles.<sup>[14]</sup> Several reports have been published with the aim to quantify binding interactions on these complex interface systems. For instance, interactions of gold nanoparticles with various host and guest systems have been determined by using cyclic voltammetry,<sup>[15]</sup> isothermal titration calorimetry,<sup>[16]</sup> and single-molecule force spectroscopy.<sup>[17]</sup>

In this work, for the first time we utilize Hamilton receptor and cyanurate guest molecules to study the host-guest interactions on the surface of functionalized SPIONs (Scheme 1). We prepare two types of nanoparticles bearing either the Hamilton receptor ( $\text{Fe}_3\text{O}_4@$ HamPac) or the cyanurate derivative ( $\text{Fe}_3\text{O}_4@$ CyaPac) and investigate how the position of the interacting molecules affects the overall binding events on the surface. We also introduce bulky hexabenzocoronene (HBC) subunits into the molecules placed in solution to investigate their effect on the affinity of nanoparticles.

The phosphonic acid derivatives of Hamilton receptors (HamPac) and cyanurate molecules (CyaPac) were prepared



**Scheme 1.** Surface modification of superparamagnetic iron oxide ( $\text{Fe}_3\text{O}_4$ ) nanoparticles (SPIONs) with cyanurate phosphonic acid CyaPac and Hamilton receptor phosphonic acid HamPac, and the general representation of explored host-guest interactions on the surface of nanoparticles.

## Results and Discussion

### Synthesis of functionalized receptors and guest molecules

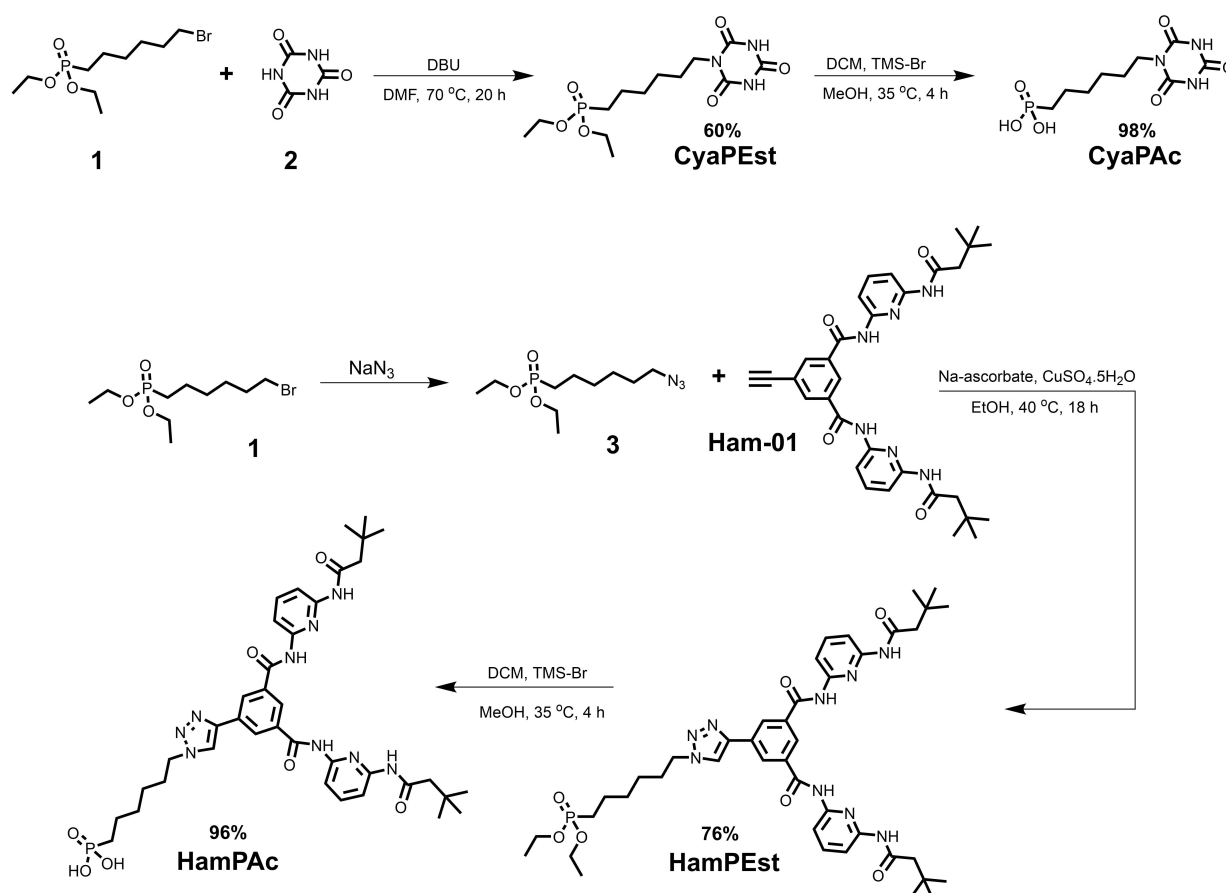
The general synthesis of functionalized receptor and guest molecules is shown in Scheme 2. The phosphonic acid moieties are known to have high affinity to the surface of metal oxides.<sup>[18]</sup> The cyanurate phosphonic acid conjugate **CyaPAC** was prepared as reported before with a slight modification at the last deprotection step. Hamilton receptor - phosphonic acid conjugate **HamPAC** was prepared by using the click reaction starting from the literature known ethynyl Hamilton receptors **Ham-01**.<sup>[12a]</sup>

First, bromo hexyl phosphonate ester (**1**) was reacted with cyanuric acid (**2**) in the presence of DBU as a base resulting in cyanurate phosphonate ester **CyaPEst**. The phosphonate ester was subsequently deprotected by TMS-Br to yield the cyanurate phosphonic acid conjugate **CyaPAC**. The formation of the product was proved by <sup>31</sup>P NMR data showing one signal at 31.90 ppm in DMSO-*d*<sub>6</sub>. After deprotection, the phosphorus signal shifts to 26.46 ppm (Supporting Information, Figure S9&S12). <sup>13</sup>C NMR data was also in agreement with the proposed structure (Supporting Information, Figure S8&S11). To prepare Hamilton receptors, bromo hexyl phosphonate **1** was converted to azide **3** - a precursor for the click reaction with

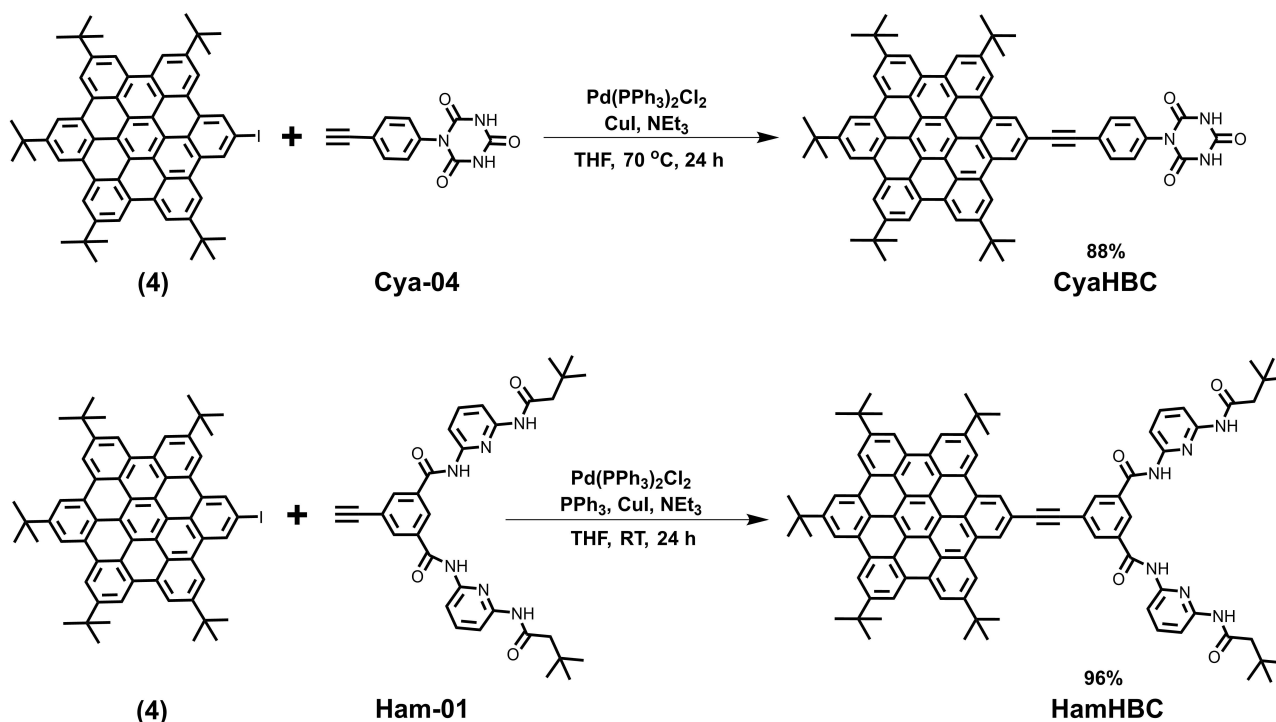
Hamilton receptor **Ham-01**. Receptors **HamPEst** was then converted to phosphonic acid **HamPAC** via a deprotection reaction by using TMS-Br (Scheme 2).

The ester derivatives **HamPEst** and **CyaPEst** have better solubility in many chlorinated and polar aprotic solvents like chloroform and DMSO, while the acid derivatives are soluble only in polar aprotic solvents like DMSO or THF, which containing oxygen atoms. Since association of Hamilton receptors with cyanurate guests rely on hydrogen bonding interactions, the choice of solvents is crucial to achieve strong binding. Hydrogen bonds are weak in polar solvents, while in chlorinated solvents, they can be maximized. These effects can be seen when the **HamPEst** is dissolved in various deuterated solvents (Supporting Information, Figure S21). In CDCl<sub>3</sub> and ACN-*d*<sub>3</sub>, the protons of active sites appear in lower frequency, while DMSO strongly solvates NH-sites and thus hamper the interaction.

Two sets of complementary molecules containing HBC were synthesized (Scheme 3). Receptor **HamHBC** was prepared via general Sonogashira coupling pathway using ethynyl Hamilton receptor **Ham-01** and iodo-HBC (**4**) as the precursors. In the similar manner, **CyaHBC** was prepared using iodo-HBC (**4**) and ethynyl cyanurate derivative **Cya-04** to give the desired product in a very good yield. Both molecules, **HamHBC** and **CyaHBC**, have similar absorption features in dichlorobenzene (DCB)



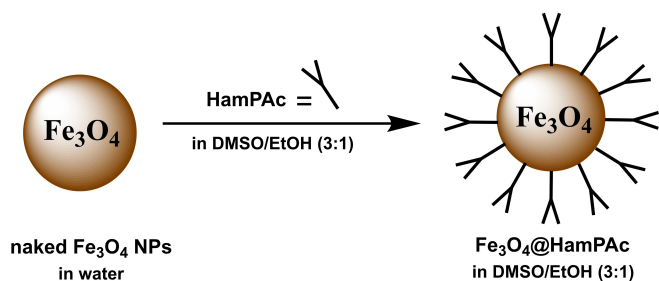
**Scheme 2.** Synthesis of cyanurate phosphonic acid **CyaPAC** and Hamilton receptor phosphonic acid **HamPAC** via the click chemistry route.



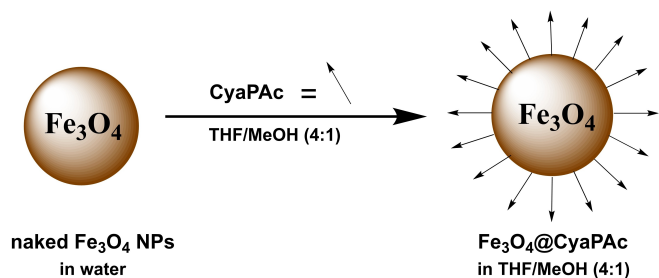
Scheme 3. Synthesis route of hexabenzocoronene derivative molecules of CyahBC and HamHBC via Sonogashira coupling reactions.

having HBC oscillation features at wavelength ranging from 350 to 420 nm, and for the HamHBC molecules there is a distinct

absorption band at 305 nm belongs to the Hamilton receptor moieties (Supporting Information, Figure S23 and S24).



Scheme 4. Functionalization process of pristine  $\text{Fe}_3\text{O}_4$  NPs with Hamilton receptor phosphonic acid conjugate **HamPac** in the solvent mixture of DMSO/EtOH (3:1).



Scheme 5. Functionalization process of pristine  $\text{Fe}_3\text{O}_4$  NPs with cyanurate phosphonic acid **CyaPac** to form  $\text{Fe}_3\text{O}_4$ @**CyaPac** in a THF/MeOH (4:1) solvent mixture.

#### Functionalization of SPIONs

For surface modification processes, commercially available SPIONs from Plasmachem™ with average size  $8 \pm 3$  nm were used. The SPIONs were stabilized in aqueous dispersion without any organic stabilizer and have initial concentration of 30 mg/mL. The naked pristine SPIONs were functionalized by mixing with corresponding receptors or guests in suitable solvent mixtures (Scheme 4 and Scheme 5). The staggering concentrations of hosts or guests was used to obtain the saturation condition of monolayer functionalization yielding a clear brownish dispersion of modified SPIONs. The dried functionalized SPIONs were characterized and used further as a dispersion in desirable solvents.

For monolayer functionalization, six dispersions of SPIONs with concentration of 1.25 mg/mL were prepared and mixed with the organic ligands of **HamPac** in DMSO/EtOH (3:1) solvent mixture. From samples 1 to 6, the concentration of **HamPac** ligands was varied between 1 to 15 mM to saturate the monolayer functionalization. Then, the mixtures were sonicated and centrifuged. After washing twice in dried ethanol to remove the excess unbound ligands, the functionalized  $\text{Fe}_3\text{O}_4$ @**HamPac** nanoparticles were dried at 75 °C overnight. Subsequently, the dried  $\text{Fe}_3\text{O}_4$ @**HamPac** nanoparticles can be redispersed in suitable organic solvents for further use.

From the FTIR spectroscopy measurements, the functionalized nanoparticles with **HamPAC** molecules show new bands at wavenumber 2950 ( $-\text{CH}_3$ ), 1650 ( $\text{C}=\text{O}$  and  $\text{C}=\text{N}$  vibrations), 1443 ( $\text{C}-\text{H}$  deformation), 1235 ( $\text{P}=\text{O}$ ), and 1035 ( $\text{P}-\text{O}$ )  $\text{cm}^{-1}$  (Figure 1a), indicating the presence of Hamilton receptors anchored to the surface of SPIONs. Furthermore, from TGA results (Figure 1b), the mass loss can be observed starting at heating temperature 300 °C till 420 °C. By plotting the mass loss against the used concentrations, the saturation condition was observed at ligand concentration of 15 mM with mass loss about 12% (Figure 1c). Using this information, the grafting density ( $\theta$ ) at saturated monolayer functionalization was determined to be about 0.73 molecules/ $\text{nm}^2$ . This value corresponds to approximately 150 Hamilton receptors attached on the surface of single SPION (see Supporting Information: Functionalization of Nanoparticles).

The size distributions of  $\text{Fe}_3\text{O}_4$ @**HamPAC** nanoparticles in solvent mixture of DMSO/EtOH (3:1) were measured using DLS at concentration of 0.2 mg/mL. At lowest concentration of applied Hamilton receptor solutions, the average size was about 8 nm, which is close to the size of the solid core of SPIONs obtained by TEM (Figure 1f). In the presence of excess of the receptor, the average size of  $\text{Fe}_3\text{O}_4$ @**HamPAC** nanoparticles in dispersion was about 15 nm (Figure 1d). The zeta potential values were positive but decreased along with the increase of applied concentration of Hamilton receptor ligands (Figure 1e).

From about 45 nm in pristine form, the zeta potential was dropped to 22 mV at the saturated condition.

Following similar procedure, the solvent mixture THF/MeOH (4:1) was used to perform functionalization of SPIONs with cyanurate phosphonic acids **CyaPAC** molecules to yield a saturated monolayer functionalization. After the functionalization process, the  $\text{Fe}_3\text{O}_4$ @**CyaPAC** nanoparticles were characterized and redispersed in suitable organic solvents. The FTIR spectroscopy (Figure 2a) showed several bands at 1690, 1460 and 1018  $\text{cm}^{-1}$ , which correspond to molecular vibrations of ( $\text{C}=\text{O}$ ) carbonyl, ( $\text{O}=\text{C}-\text{NH}-$ ) amide, ( $\text{CH}_2-$ ) alkyl chain, and ( $\text{P}-\text{O}$ ) alkyl phosphite groups. Furthermore, a significant mass loss was observed on heating temperature in the range 320–380 °C (Figure 2b), which originates from decomposition of cyanurate ligands on the surface of modified SPIONs. From TGA measurements, modified  $\text{Fe}_3\text{O}_4$ @**CyaPAC** nanoparticles reached the saturation at 9.5% of mass loss using 20 mM ligand concentration (Figure 2c). Under these conditions, the surface of SPIONs was covered with **CyaPAC** monolayer with grafting density of 1.5 molecule/ $\text{nm}^2$ . Thus, at saturation, there are approximately 300 **CyaPAC** molecules anchored to the surface of a single particle of SPION, which is double of the number of attached Hamilton receptor molecules (see Supporting Information: Functionalization of Nanoparticles). According to the DLS measurements of  $\text{Fe}_3\text{O}_4$ @**CyaPAC**, nanoparticles have the average size of 48 nm at saturated conditions (Figure 2d). This data indicates that functionalized  $\text{Fe}_3\text{O}_4$ @**CyaPAC** nanoparticles clus-

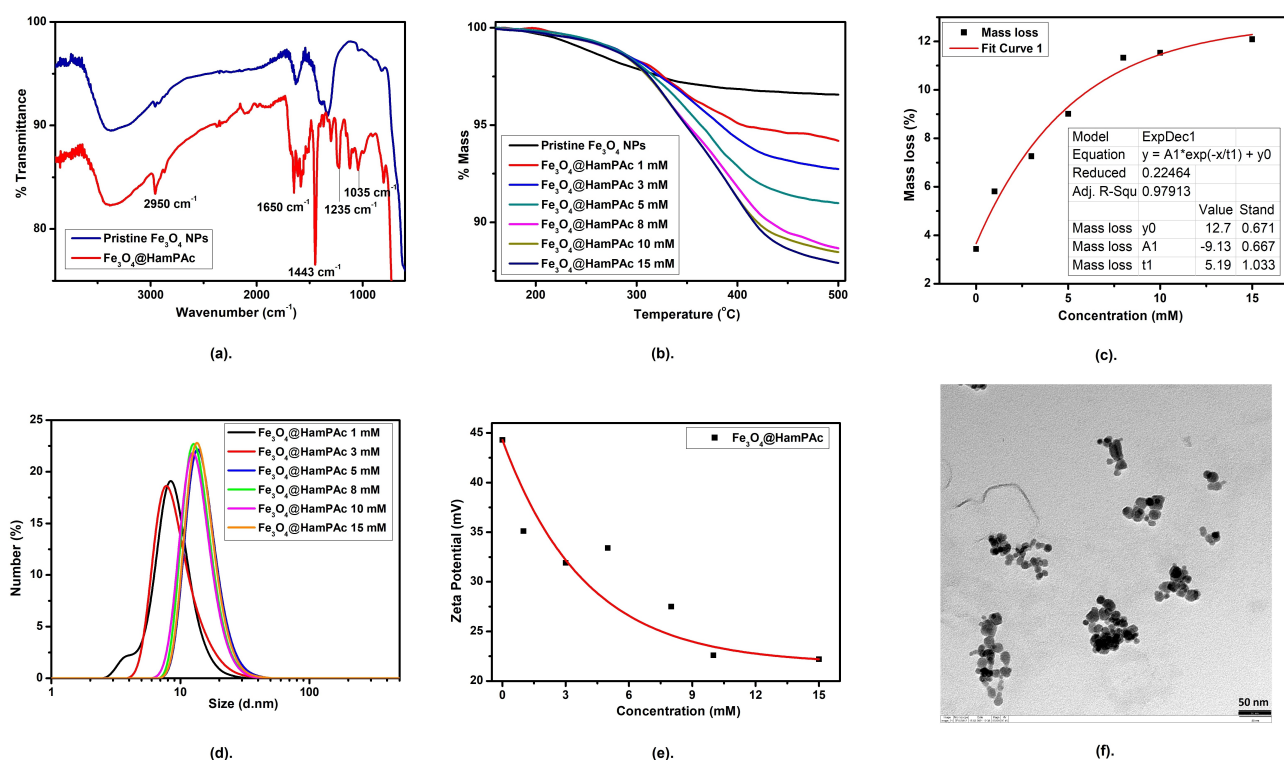


**Figure 1.** (a) FTIR spectra of pristine  $\text{Fe}_3\text{O}_4$  NPs (blue) and post functionalized  $\text{Fe}_3\text{O}_4$ @**HamPAC** (red), (b) TGA curve: %mass versus **HamPAC** concentration added during functionalization process, (c) plot of %mass loss as a function of added **HamPAC** showing the saturation at about 12% of mass loss, (d) size distributions from DLS measurement stated in number (%), and (e) zeta potential of  $\text{Fe}_3\text{O}_4$ @**HamPAC** measured in DMSO/EtOH (3:1) showing a trend of decreasing values, (f) TEM picture of functionalized  $\text{Fe}_3\text{O}_4$ @**HamPAC**.

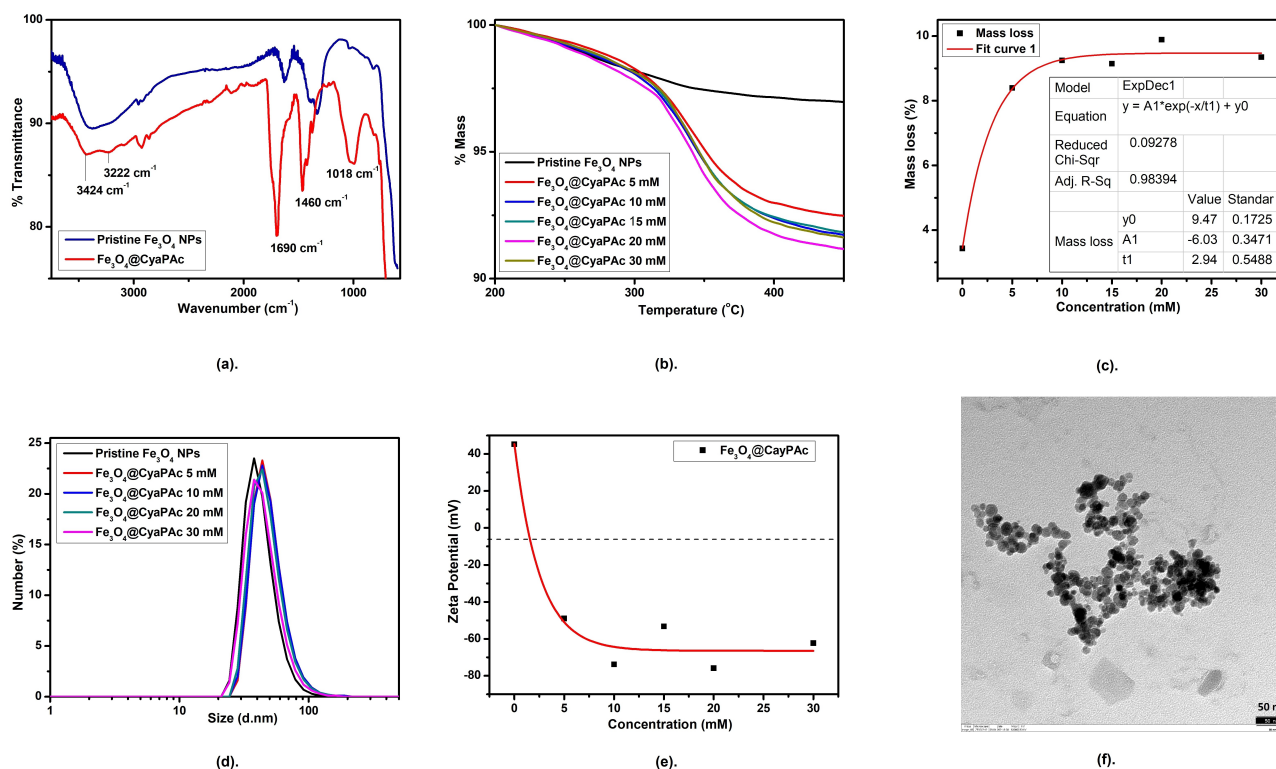


**Figure 2.** (a) FTIR spectra of pristine  $\text{Fe}_3\text{O}_4$  NPs (blue) and post functionalized  $\text{Fe}_3\text{O}_4@CyaPac$  (red), (b) %mass of TGA curve versus **CyaPac** concentration adding during functionalization process, (c) plot of %mass loss as a function of added **CyaPac** concentration showing the plateau of %mass loss at about 9.5%, (d) size distributions from DLS measurement stated in number (%), and (e) zeta potential of  $\text{Fe}_3\text{O}_4@CyaPac$  measured in THF/MeOH (4:1) showing a negative value, (f) TEM picture of functionalized  $\text{Fe}_3\text{O}_4@CyaPac$ .

ter together forming poly-nucleation, which has an increased average size. The zeta potential was found to be negative and reached  $-70$  mV, indicating high stability of the system in a THF/MeOH (4:1) mixture (Figure 2e). The TEM picture of  $\text{Fe}_3\text{O}_4@CyaPac$  nanoparticles showed the iron oxide cores remain intact after post functionalization (Figure 2e).

### NMR studies of host-guest interactions at the molecular level

First, we investigated the formation of complexes between receptors and guests in solution to understand the systems at the molecular level in solution. Since hydrogen bonding interactions are weak in highly polar solvents, the binding affinities of free receptors in solutions were determined in chloroform. Hamilton receptor **HamPEst** and cyanurate derivative **CyaPEst** were used as esters because of their good solubility in chloroform.

The Job's plot based on NMR data confirmed that **HamPEst** and **CyaPEst** form a 1:1 complex in  $\text{CDCl}_3$  (Supporting Information, Figure S20b&S20c). The initial chemical shift of the active protons from the **HamPEst** molecules in deuterated chloroform are at 8.46 and 8.14 ppm. After mixing with **CyaPEst**, the signals of protons are shifted downfield to 9.95 and 9.42 ppm, respectively (Figure 3b and 3c). Association constants ( $K_a = 1.25 \times 10^4 \text{ M}^{-1}$ ) of the complex between **HamP-**

**Est** and **CyaPEst** were determined from NMR data by using **BindFit** software<sup>[19]</sup>. This value is similar to the one reported by Hamilton and Chang with barbiturate molecules as a guest.<sup>[9]</sup> Thus, our functionalization does not considerably affect the binding event. Complexation of **HamHBC** with **CyaPEst** measured under the same conditions was in the same range  $4.92 \times 10^4 \text{ M}^{-1}$  (Figure 3h and 3i).

Similar NMR titrations we carried out for the complexation of **HamPEst** with **CyaHBC** in a mixture of deuterated chloroform and THF (9:1) because of better solubility of HBC-cyanurate derivatives in this solvent mixture (Figure 3e and 3f). The calculated binding constants is  $1.33 \times 10^3 \text{ M}^{-1}$ , which is slightly less value because of the presence of THF.

### Supramolecular interactions on the surface of nanoparticles

In order to study host-guest interactions on the surface, dried functionalized SPIONs were weighted and redispersed in the chlorinated solvent to prepare a desired concentration of stable dispersions (Scheme 6). To assess binding affinity of functionalized nanoparticles towards guest molecules by UV-Vis measurements, we converted the concentration of nanoparticles ( $c_{nano}$ ) to the concentration of the attached units knowing grafting density from TGA measurements. In other words, we consider nanoparticles as a solution of receptors or guests. For instance,

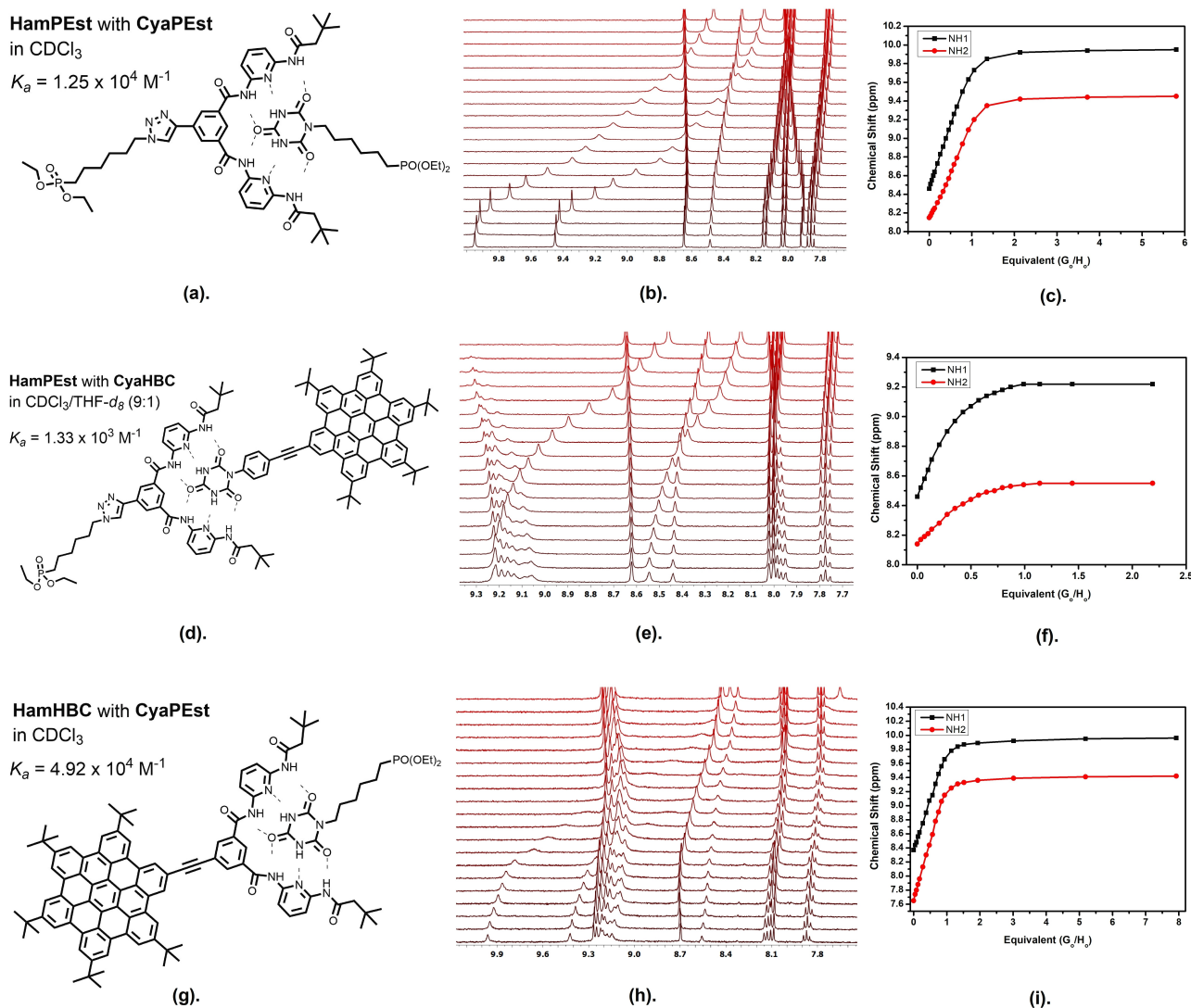
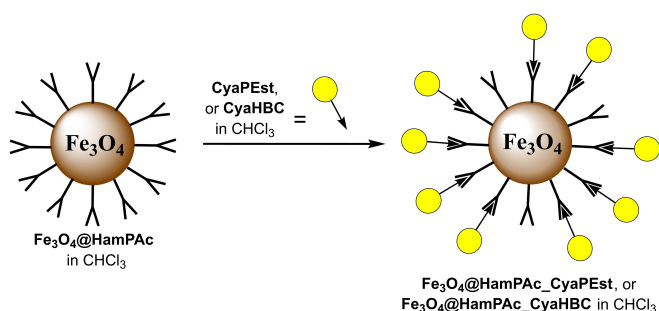


**Figure 3.** Interaction of Hamilton receptors with cyanurate guests, and the corresponding NMR titration data of (a, b, and c) **HamPEst** with **CyaPEst** molecules in  $\text{CDCl}_3$ , (d, e, and f) **HamPEst** with **CyaHBC** molecules in mixture of  $\text{CDCl}_3/\text{THF-}d_8$  (9:1), and (g, h, and i) **HamHBC** with **CyaPEst** molecules in  $\text{CDCl}_3$ .



**Scheme 6.** Schematic representation of supramolecular interactions on the surface of Hamilton receptor functionalized SPIONs  $\text{Fe}_3\text{O}_4@HamPAC$  coupled with cyanurate derivative guest molecules **CyaPEst** or **CyaHBC** in  $\text{CHCl}_3$ .

ca. 150 Hamilton receptors are attached to one nanoparticles. This corresponds to the maximum possible concentration of the Hamilton receptors in solution, which is equal to  $150 \cdot c_{nanor}$  thus

the ratio of guest to host ( $G_0/H_0$ ) in the system can be approximated. In these titration experiments, the guest molecules were dissolved in the prepared dispersion of nanoparticles, so that the concentration of nanoparticles in the system remains the same during spectroscopic titration process. Therefore, the background interferences and scattering effects from modified nanoparticles can be minimized and the binding interactions are not perturbed by the presence of SPIONs. Thus, the change of absorption features and the shift of absorption peaks were caused solely by the interactions of host-guest molecules on the surface of functionalized SPIONs.

In order to compare the interaction of host-guest systems at the molecular level and on the surface of nanoparticles, we always performed two sequential experiments with free receptors and those attached to the surface. For example, UV-Vis titration of **HamPEst** with **CyaPEst** in chloroform yielded  $\text{Log } K = 3.92 \pm 0.01 \text{ M}^{-1}$ . As can be seen in Figure 4a, the bathochromic shift from 302 to 308 nm is observed during the

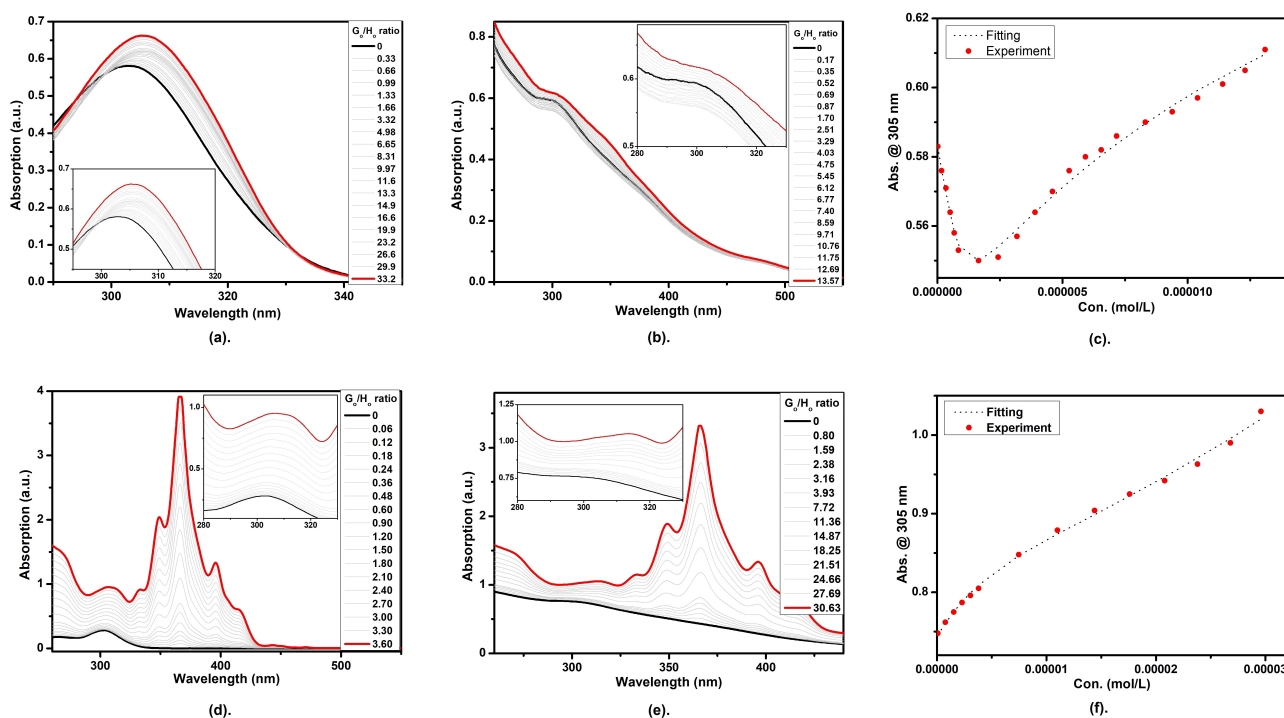


**Figure 4.** UV-Vis titration spectra of (a) free molecules in solution of **HamPEst** and **CyaPEst** molecules, as model of titration of (b) functionalized  $\text{Fe}_3\text{O}_4@$ **HamPAC** nanoparticles with **CyaPEst** in  $\text{CHCl}_3$ , while (d) titration spectra of free molecules of **HamPEst** with **CyaHBC** molecules, as model of titration of (e) functionalized  $\text{Fe}_3\text{O}_4@$ **HamPAC** nanoparticles with **CyaHBC** in  $\text{CHCl}_3$ . The fitting of titration results from  $\text{Fe}_3\text{O}_4@$ **HamPAC** with (c), **CyaPEst** molecules and with (f), **CyaHBC** molecules showing higher complexation degree.

addition of **CyaPEst**. This result is in a good agreement with our NMR titrations (Figure 3a). The association of **HamPEst** with **CyaHBC** was detected one order of magnitude stronger  $\log K = 5.10 \pm 0.02 \text{ M}^{-1}$  (Figure 4d). This is approximately two orders of magnitude stronger than the binding determined in  $\text{CDCl}_3/\text{THF}-d_6$  mixture by using NMR method. The difference in binding constants can be explained by the difference in the solvent polarity. Interestingly, the presence of HBC subunit contributes to the binding approximately one order of magnitude. Since the Hamilton receptor is a large  $\pi$ -system, we suggest that the HBC can form stacking interactions with the receptor and thus additionally stabilize the host-guest complex.

The titration experiments with functionalized SPIONs nanoparticles revealed that host-guest interactions on the surface are possible and can be easily detected by spectroscopy. The particles with the composition  $\text{Fe}_3\text{O}_4@$ **HamPAC** strongly interact with **CyaPEst** and show similar UV-Vis features as for the titration of the free receptor in solution (compare Figure 4a & Figure 4b). A pronounced increase of absorption was observed at 345 nm, indicating the interaction between the guest molecules with the Hamilton receptor on the surface of SPIONs. Analysis of the binding data by using HypSpec software reveals multiple events with apparent binding constants  $\log K_{11} = 7.05 \pm 0.01 \text{ M}^{-1}$  and  $\log K_{12} = 4.77 \pm 0.01 \text{ M}^{-1}$ , where  $K_{11}$  and  $K_{12}$  represent association constants for the 1:1 complex and 1:2 complexes, respectively (Figure 4c). This stoichiometry is not a real stoichiometry; however, it shows that the nanoparticle is able to bind more guest molecules on the surface as compared

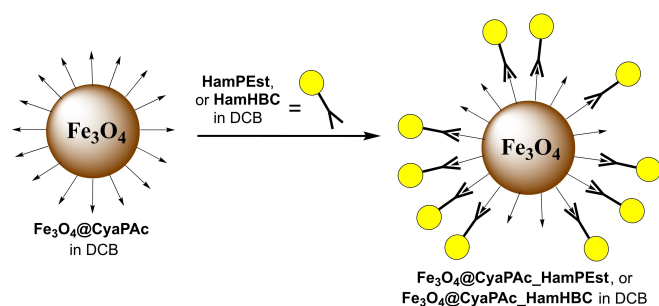
to the host-guest interaction at the molecular scale. As can be seen from the fitting analysis, the absorption drops and then increases indicating stepwise attachment of the guest to the nanoparticle. Such changes can be explained by reorganization of the receptor on the surface after binding of a certain amount of guests or the ability to coordinate more guests through any additional non-covalent interactions. The collective interactions can emerge due to the synergistic effects of complex environment on the surface of the functionalized SPIONs.

A completely different situation was observed for the titration of  $\text{Fe}_3\text{O}_4@$ **HamPAC** nanoparticles with **CyaHBC** in  $\text{CHCl}_3$ , shifting of absorption peak was observed (Figure 4e). The absorption peak of Hamilton receptors on the surface of modified SPIONs was shifted from 300 to 315 nm. The shift from supramolecular interactions on the surface of modified SPIONs is much bigger as compared to the shift between free molecules in the solution. However, the absorption feature of HBC moiety did not fundamentally change indicating that HBC moiety is not directly involved in the binding process. The fitting analysis (Figure 4f) yielded also stepwise binding but with much lower affinities:  $\log K_{11} = 3.31 \pm 0.01 \text{ M}^{-1}$  and  $\log K_{12} = 3.19 \pm 0.01 \text{ M}^{-1}$ . It is likely, that lower affinity was observed because HBC moiety is large enough to hinder efficient supramolecular interactions. On the other hand, fluorescence titration of  $\text{Fe}_3\text{O}_4@$ **HamPAC** nanoparticles with **CyaHBC** in DCB has been performed to give additional insight of the system (Supporting Information, Figure S27a&S27b). The fluorescence titration results could be fitted with 1:1 complexation ratio,



giving the binding constant of  $\log K=5.73 \pm 0.01 \text{ M}^{-1}$  which show similar order of magnitude to that obtained by using UV/Vis method.

In the next series of experiments, we inverted the interaction pattern by attaching cyanurate acid derivative to the nanoparticles, while the Hamilton receptor was in solution. The big difference to the previous case is the fact that nanoparticles contain approximately 300 **CyaPac** molecules, which is double than the Hamilton receptor molecules on the surface. This difference arose because the cyanurate acid derivative is smaller in size resulting in higher grafting density on the surface of functionalized SPIONs. For solubility reasons we changed the solvent systems to DCB (Scheme 7).



**Scheme 7.** Schematic representation of supramolecular interactions on the surface of cyanurate derivative functionalized SPIONs  $\text{Fe}_3\text{O}_4\text{@CyaPac}$  coupled with Hamilton receptor molecules **HamPEst** or **HamHBC** in dichlorobenzene (DCB).

The UV-Vis titration of free receptor **HamPEst** with **CyaPEst** in DCB resulted in  $\log K=4.35 \pm 0.01 \text{ M}^{-1}$ . We also observed a small bathochromic shift upon the complexation (Figure 5a). Furthermore, the titration of **HamHBC** with **CyaPEst** resulted in similar association constant:  $\log K=4.63 \pm 0.01 \text{ M}^{-1}$  (Figure 5d). The result is similar with the NMR titration measurements of the same complex. Moreover, the absorption peak of Hamilton receptors was increased and shifted from 305 to 314 nm, while the absorption feature of HBC moiety remained the same.

The investigation of supramolecular interactions on the surface of cyanurate functionalized SPIONs were done by titrating Hamilton receptors to the dispersion of  $\text{Fe}_3\text{O}_4\text{@CyaPac}$  nanoparticles in DCB. Since we kept the concentration of nanoparticles constant during the titrations, the change of the absorption features upon guest addition should be only due to the host-guest complex formation on the surface of nanoparticles. When the  $\text{Fe}_3\text{O}_4\text{@CyaPac}$  nanoparticles titrate with **HamPEst** molecules, absorption peak at 337 nm emerged along with the increase of added Hamilton receptors to the dispersion (Figure 5b). This emerging absorption peak in the dispersion system is in contrast with the system using free molecules in the DCB solution where the absorption peak appeared at 304 nm. The shift of absorption peak to higher wavelength can be explained due to the complex environment of the surface of  $\text{Fe}_3\text{O}_4\text{@CyaPac}$  nanoparticles. The slight increase of absorption peak at around 340 nm was also noticed from the previous measurements when functionalized  $\text{Fe}_3\text{O}_4\text{@HamPac}$  nanoparticles titrated with cyanurate **CyaPEst** molecules in  $\text{CHCl}_3$

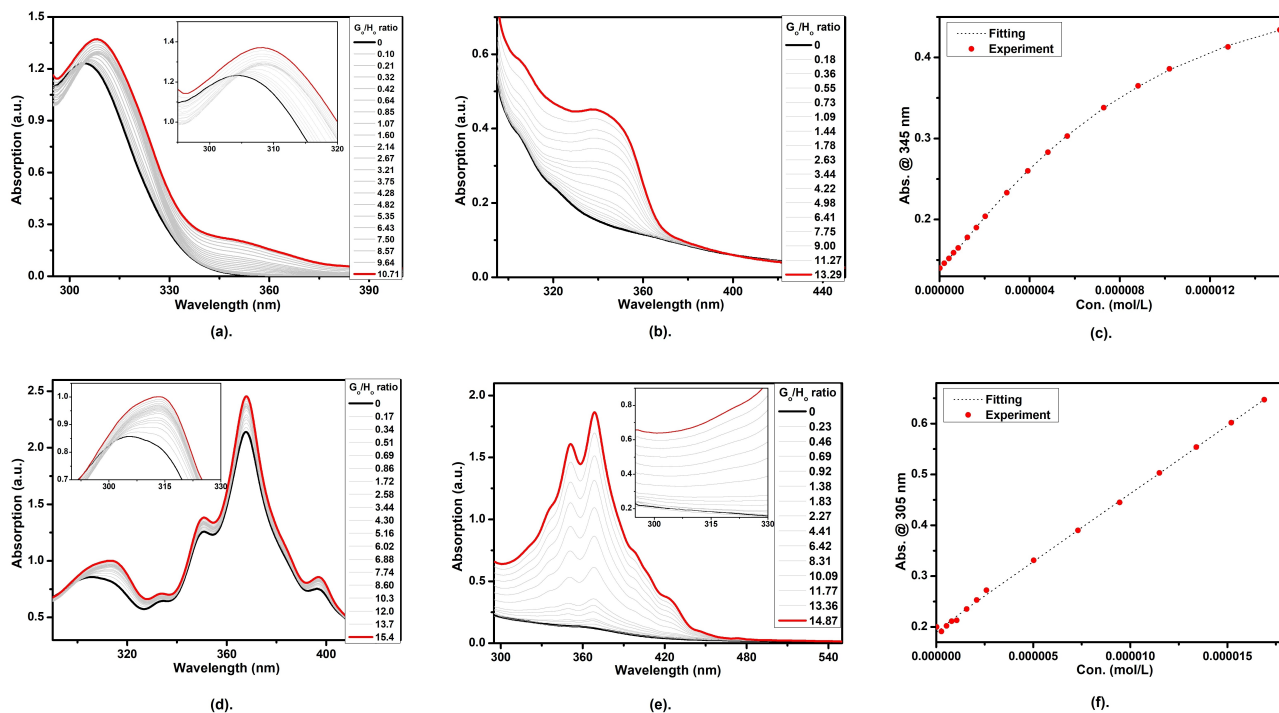


**Figure 5.** UV-Vis titration spectra of (a) **HamPEst** with **CyaPEst** in DCB, as a model of titration of (b) functionalized  $\text{Fe}_3\text{O}_4\text{@CyaPac}$  nanoparticles with **HamPEst** in DCB. (d) Titration spectra of **HamHBC** with **CyaPEst** in  $\text{CHCl}_3$ , as a model of (e) titration of functionalized  $\text{Fe}_3\text{O}_4\text{@CyaPac}$  nanoparticles with **HamHBC** in DCB. The fitting of the experimental data is presented for the titration of  $\text{Fe}_3\text{O}_4\text{@CyaPac}$  with (c) **HamPEst** and with (f) **HamHBC**.

(Figure 4b). The fitted titration resulted in  $\log K_{11}=6.73 \pm 0.01 \text{ M}^{-1}$  and  $\log K_{12}=4.65 \pm 0.01 \text{ M}^{-1}$  (Figure 5c).

Similar titration experiment of nanoparticles we performed with the addition of **HamHBC** bearing large HBC moiety. As can be seen in Figure 5e and 5f the HBC absorption pattern looks different from the titration at the molecular scale (Figure 5b). This difference implies additional interactions on the surface of functionalized nanoparticles. High binding affinity obtained from titration ( $\log K_{a1}=6.91 \pm 0.02 \text{ M}^{-1}$ ) supports the suggestion that HBC moieties can interact with each other and additionally stabilize the coordination. Additional measurement of fluorescence titration among **Fe<sub>3</sub>O<sub>4</sub>@CyaPac** nanoparticles with **HamHBC** molecules has been performed. The results can be fitted with 1:1 complexation ratio showing binding constant of  $\log K=5.10 \pm 0.02 \text{ M}^{-1}$  (Supporting Information, Figure S28a&S28b).

## Conclusion

We have designed and synthesized a series of new functionalized nanoparticles SPIONs bearing complementary hydrogen bonding subunits: the Hamilton receptors and cyanurate derivatives. The host-guest interactions have been studied in detail at the molecular level and on the surface of nanoparticles. We have varied the position of the Hamilton receptor and cyanurate derivatives either in solution or on the surface of the nanoparticles. Two type of nanoparticles were successfully prepared **Fe<sub>3</sub>O<sub>4</sub>@HamPac** and **Fe<sub>3</sub>O<sub>4</sub>@CyaPac**. The latter type is packed with approximately double more molecules than the first one, because of the smaller size of cyanurates. HBC-based guests were designed to investigate their effect on surface binding. It was found that collective hydrogen bonding interaction on the surface is approximately three orders of magnitude stronger as compared to similar interactions of the corresponding compounds in solution at the molecular scale. The effect of positioning the Hamilton receptor on the surface or in the solution is minimal. Both types of nanoparticles showed similar affinities according to the UV-Vis titration experiments. Interestingly, the effect of bulky HBC appeared to be different. Binding of **CyaHBC** to **Fe<sub>3</sub>O<sub>4</sub>@HamPac** was hampered, while coordination of **HamHBC** to **Fe<sub>3</sub>O<sub>4</sub>@CyaPac** was stabilized, even though this type of particles has more dense packing. As revealed from the titration analysis, each receptor molecule on the surface can coordinate more than one guests from the solution. These studies are fundamentally important to give a better insight into the supramolecular complexations on hybrid organic-inorganic systems, offering deeper potential applications in areas such as nanomaterials, nanosensing devices, and drug delivery systems.

## Experimental Section

**General method and procedures:** pristine superparamagnetic iron oxide (Fe<sub>3</sub>O<sub>4</sub>) nanoparticles were purchased from PlasmaChem as aqueous suspension without any organic stabilizer, average particle size  $8 \pm 3 \text{ nm}$  and weight concentration 3%.

**Functionalization of Fe<sub>3</sub>O<sub>4</sub>@CyaPac:** Fe<sub>3</sub>O<sub>4</sub>-NPs from stock solution with concentration of 30 mg/mL was taken out 1 mL and dispersed in 23 mL solution mixture of THF/MeOH (4:1) to gain the final concentration of 1.25 mg/mL in total 24 mL volume. The dispersion was sonicated for 15 minutes at 20 °C to homogenize it. Then the dispersion was divided equally into 6 centrifugation glass tube, each tube contains 5 mg of NPs from 4 mL dispersion (1.25 mg/mL). Then the NPs were centrifugated at 12500 g for 1 h at 20 °C. The supernatant was decanted and the residues were mixed with the phosphonic acid cyanurate solutions accordingly to perform functionalization process. Functionalization process was done by mixing the Fe<sub>3</sub>O<sub>4</sub>-NPs with phosphonic acid cyanurate solutions. Prior to this step, the phosphonic acid cyanurate was prepared in 6 different concentration in THF/MeOH (4:1) solution mixture to yield certain concentration. After that, the cyanurate combined with Fe<sub>3</sub>O<sub>4</sub>-NPs dispersions were sonicated for 15 minutes at 20 °C, followed by centrifugation at 12500 g for 1 h at 20 °C. The supernatant was decanted and the residue was subsequently washed two more times to get rid out the excess unbound cyanurate molecules. The washing cycle was done by dispersing the NPs residue in 4 mL THF/MeOH (4:1) mixture, then sonicated for 15 minutes at 20 °C, followed by centrifugation at 12500 g for 1 h at 20 °C. After decantation of the solution, the final functionalized Fe<sub>3</sub>O<sub>4</sub>-NPs are dried in the drying oven for overnight at 75 °C to get solid cyanurate functionalized Fe<sub>3</sub>O<sub>4</sub>-NPs that can be dispersed accordingly and used further.

**Functionalization Fe<sub>3</sub>O<sub>4</sub>@HamPac:** Fe<sub>3</sub>O<sub>4</sub>-NPs from stock solution with concentration of 30 mg/mL was taken out 1 mL and dispersed in 23 mL solution mixture of DMSO/EtOH (3:1) to gain the final concentration of 1.25 mg/mL in total 24 mL volume. The dispersion was sonicated for 15 minutes at 20 °C to homogenize it. Then the dispersion was divided into 6 centrifugation glass tube, each tube contains 5 mg of NPs from 4 mL dispersion (1.25 mg/mL). Then the NPs were centrifugated at 12500 g for 1 h at 10 °C. The supernatant was decanted and the residues were mixed with the phosphonic acid Hamilton receptor solutions accordingly to perform functionalization process. Functionalization process was done by mixing the Fe<sub>3</sub>O<sub>4</sub>-NPs with phosphonic acid Hamilton receptor solutions. Prior to this step, the phosphonic acid Hamilton receptor was prepared in 6 different concentration in DMSO/EtOH (3:1) solution mixture to yield certain concentration. After that, the Hamilton receptor combined with Fe<sub>3</sub>O<sub>4</sub>-NPs dispersions were sonicated for 15 minutes at 20 °C, followed by centrifugation at 12500 g for 1 h at 10 °C. The supernatant was decanted and the residue was subsequently washed twice to get rid out the excess unbound cyanurate molecules. The washing cycle was done by dispersing the NPs residue in 4 mL dried EtOH, then sonicated for 15 minutes at 20 °C, followed by centrifugation at 12500 g for 1 h at 10 °C. After decantation of the solution, the final functionalized Fe<sub>3</sub>O<sub>4</sub>-NPs are dried in the drying oven for overnight at 75 °C to get solid Hamilton receptor functionalized Fe<sub>3</sub>O<sub>4</sub>-NPs that can be dispersed accordingly and used further.

## Acknowledgements

We thank fully the Cluster of Excellence “Engineering of Advanced Material” (EAM) and the Graduate School Advanced Material and Processes (GS AMP) for financial support. Open Access funding enabled and organized by Projekt DEAL.

## Conflict of Interest

The authors declare no conflict of interest.

**Keywords:** artificial hydrogen bonds · functionalized nanoparticles · hamilton receptors · host-guest chemistry · SPIONs

- [1] a) L. Mohammed, H. G. Gomaa, D. Ragab, J. Zhu, *Particuology* **2017**, *30*, 1–14; b) K. Ulbrich, K. Holá, V. Šubr, A. Bakandritsos, J. Tuček, R. Zbořil, *Chem. Rev.* **2016**, *116*, 5338–5431.
- [2] a) T. Luchs, P. Lorenz, A. Hirsch, *ChemPhotoChem* **2020**, *4*, 52–58; b) Q. M. Kainz, O. Reiser, *Acc. Chem. Res.* **2014**, *47*, 667–677.
- [3] a) S. Lata, S. R. Samadder, *J. Environ. Manage.* **2016**, *166*, 387–406; b) H. Park, A. May, L. Portilla, H. Dietrich, F. Münch, T. Rejek, M. Sarcletti, L. Banspach, D. Zahn, M. Halik, *Nat. Sustain.* **2020**, *3*, 129–135; c) M. Sarcletti, D. Vivod, T. Luchs, T. Rejek, L. Portilla, L. Müller, H. Dietrich, A. Hirsch, D. Zahn, M. Halik, *Adv. Funct. Mater.* **2019**, *29*, 1805742.
- [4] a) A. K. Gupta, M. Gupta, *Biomaterials* **2005**, *26*, 3995–4021; b) A. V. Samrot, C. S. Sahithya, J. Selvarani, A. S. K. Purayil, P. Ponnaiah, *Curr. Res. Green Sustain. Chem.* **2021**, *4*, 100042.
- [5] a) S. Kralj, D. Makovec, S. Čampelj, M. Drofenik, *J. Magn. Magn. Mater.* **2010**, *322*, 1847–1853; b) C. G. C. M. Netto, H. E. Toma, L. H. Andrade, *J. Mol. Catal. B* **2013**, *85–86*, 71–92.
- [6] A. K. Peacock, S. I. Cauët, A. Taylor, P. Murray, S. R. Williams, J. V. M. Weaver, D. J. Adams, M. J. Rosseinsky, *Chem. Commun.* **2012**, *48*, 9373–9375.
- [7] S. S. Khasraghi, A. Shojaei, U. Sundararaj, *Mater. Sci. Eng. C* **2020**, *114*, 110993.
- [8] S. Zhao, X. Yu, Y. Qian, W. Chen, J. Shen, *Theranostics* **2020**, *10*, 6278–6309.
- [9] S. K. Chang, A. D. Hamilton, *J. Am. Chem. Soc.* **1988**, *110*, 1318–1319.
- [10] F. Wessendorf, J. F. Gnichwitz, G. H. Sarova, K. Hager, U. Hartnagel, D. M. Guldi, A. Hirsch, *J. Am. Chem. Soc.* **2007**, *129*, 16057–16071.
- [11] A. Tron, P. J. Thornton, M. Rocher, H. P. J. de Rouville, J. P. Desvergne, B. Kauffmann, T. Buffeteau, D. Cavagnat, J. H. R. Tucker, N. D. McClenaghan, *Org. Lett.* **2014**, *16*, 1358–1361.
- [12] a) F. Wessendorf, A. Hirsch, *Tetrahedron* **2008**, *64*, 11480–11489; b) W. H. Binder, R. Zirbs, F. Kienberger, P. Hinterdorfer, *Polym. Adv. Technol.* **2006**, *17*, 754–757.
- [13] G. M. Kuhl, D. T. Seidenkranz, M. D. Pluth, D. W. Johnson, S. A. Fontenot, *Sensing Bio-Sensing Res.* **2021**, *31*, 100397.
- [14] a) M. Ali, D. H. Hasenöhr, L. Zeininger, A. R. M. Müllner, H. Peterlik, A. Hirsch, *Helv. Chim. Acta.* **2019**, *102*, e1900015; b) L. Zeininger, M. Klauunzner, W. Peukert, A. Hirsch, *Int. J. Mol. Sci.* **2015**, *16*, 8186–8200; c) W. H. Binder, R. Sachsenhofer, C. J. Straif, R. Zirbs, *J. Mater. Chem.* **2007**, *17*, 2125–2132.
- [15] A. Labande, J. Ruiz, D. Astruc, *J. Am. Chem. Soc.* **2002**, *124*, 1782–1789.
- [16] G. Y. Tonga, T. Mizuhara, K. Saha, Z. W. Jiang, S. Hou, R. Das, V. M. Rotello, *Tetrahedron Lett.* **2015**, *56*, 3653–3657.
- [17] M. Y. Zhang, Z. J. Gong, W. S. Yang, L. Q. Jin, S. M. Liu, S. Chang, F. Liang, *ACS Appl. Nano Mater.* **2020**, *3*, 4283–4291.
- [18] a) S. P. Pujari, L. Scheres, A. T. M. Marcellis, H. Zuilhof, *Angew. Chem. Int. Ed.* **2014**, *53*, 6322–6356; *Angew. Chem.* **2014**, *126*, 6438–6474; b) L. Zeininger, L. Portilla, M. Halik, A. Hirsch, *Chem. Eur. J.* **2016**, *22*, 13506–13512.
- [19] a) D. B. Hibbert, P. Thordarson, *Chem. Commun.* **2016**, *52*, 12792–12805; b) P. Thordarson, *Chem. Soc. Rev.* **2011**, *40*, 1305–1323.

Manuscript received: July 16, 2021

Accepted manuscript online: October 15, 2021

Version of record online: October 27, 2021